High-energy magnon dispersion demonstrate extended interactions in the undoped cuprates

M. Guarise[1], B. Dalla Piazza[1], M. Moretti Sala[2], G. Ghiringhelli[2], L. Braicovich[2], H. Berger[1], J.N. Hancock[3], D. van der Marel[3], T. Schmitt[4], V.N. Strocov[4], L.J.P. Ament[5], J. van den Brink[5], P.-H. Lin[1], P. Xu[1], H. M. Rønnow[1], and M. Grioni[1]

[1] *Institute of Condensed Matter Physics, Ecole Polytechnique Fédérale de Lausanne (EPFL), CH-1015, Switzerland*

[2] *CNR/INFM Coherentia and Soft, Dipartimento di Fisica, Politecnico di Milano, I-20133 Milano, Italy*

[3] *Institut de Physique de la Matière Condensée, 24 quai Ernest-Ansermet, Université de Genève, CH-1211, Switzerland*

[4] *Swiss Light Source, Paul Scherrer Institut, CH-5232 Villigen PSI, Switzerland and*

[5] *Intitute-Lorentz for Theoretical Physics, Universiteit Leiden, NL-2300 RA Leiden, The Netherlands*

(Dated: April 15, 2010)

Using high-resolution resonant inelastic x-ray scattering (RIXS), we performed a momentum-resolved study of magnetic excitations in the model spin-1/2 2D antiferromagnetic insulator $Sr_2CuO_2Cl_2$. We identify both a single-spin-wave feature and a multi-magnon continuum, and show that the X-ray polarization can be used to distinguish these two contributions in the cross-section. The spin-waves display a large (70 meV) dispersion between the zone-boundary points (π,0) and (π/2,π/2). Employing an extended t-t'-t''-U one-band Hubbard model, we find significant electronic hopping beyond nearest-neighbor Cu ions. We conclude that sizeable extended magnetic interactions are present in $Sr_2CuO_2Cl_2$ and probably important in all undoped cuprates.

Magnetism in the layered cuprates continues to be a subject of considerable interest, in relation to both the fundamental quest to understand strong electron correlation and quantum spin effects in Mott insulators, and to the search for the mechanism of high-T_c superconductivity. To lowest order, the undoped cuprates can be described by the simple nearest neighbor (NN) antiferromagnetic Heisenberg model, but it has been argued on the basis of high-energy inelastic neutron scattering (INS) data on La_2CuO_4 (LCO) [1] that further neighbor magnetic interactions are present. To disentangle generic behavior from properties depending on the chemical structure of specific materials, it is therefore important to investigate the excitation spectrum in other members of the cuprate family. In this Letter we report resonant inelastic x-ray scattering (RIXS) results on the magnetic excitation spectrum of the compound $Sr_2CuO_2Cl_2$ (SCOC). We discover a surprisingly large dispersion along the magnetic Brillouin zone (MBZ) boundary. An analysis of the data in terms of an extended Hubbard model demonstrate and quantify the existence of sizeable further neighbor electronic hopping. Our results imply that a series of longer-ranged magnetic interactions are present in SCOC and probably generally important in the cuprates.

SCOC is an insulating single-layer parent compound of the high-T_c superconducting (SC) materials. It is isostructural to the high-temperature tetragonal phase of La_2CuO_4 (LCO), with La replaced by Sr, and the apical oxygen ions of the CuO_6 octahedra replaced by Cl. AFM order develops below T_N=256 K with a reduced Cu moment of 0.34 μ_B, and the Cu spins aligned along the (110) direction in the CuO_2 plane, at 45° from the Cu-O bonds. Both the in-plane (XY) anisotropy and the interlayer coupling are very small. SCOC remains tetragonal down to low temperature, and the distance between adjacent CuO_2 planes is 18% larger than in LCO. For all these reasons SCOC is an almost ideal realization of an S=1/2 2D square-lattice Heisenberg AFM [2].

Magnetic excitations in SCOC have been identified in optical, Raman, and inelastic neutron scattering (INS) data. A structure at 0.35 eV in the absorption coefficient [3] is interpreted as a quasi-bound state of two magnons (a bimagnon) assisted by a phonon with momentum $Q_{ph} \sim (\pi,0)$ [4]. Two-magnon excitations at E_{2M}=0.35 eV in the Raman spectra suggest a superexchange energy $J \sim 0.13$ eV [5, 6]. Neither Raman nor optics are sensitive to single magnons, which are optically-forbidden spin-flip (ΔS=1) excitations. INS is the natural probe of magnons, but the large J, and the difficulty of obtaining large single crystals, are major experimental obstacles. The full magnon spectrum of a cuprate has only been reported for LCO [1]. A $\sim$ 20 meV dispersion was found along the MBZ boundary, implying magnetic interactions extending beyond NN Cu spins. INS measurements of SCOC have so far been limited to low energies, therefore covering only small Q around the ordering wave vector [7].

Resonant inelastic x-ray scattering (RIXS) [8] is the x-ray counterpart of resonant optical Raman spectroscopy, with important specificities: i) a core hole in the intermediate states enforces chemical selectivity; ii) the x-ray photon carries a momentum comparable to the size of the BZ, so that RIXS is not limited to Q=0 excitations; iii) when performed at the $L_{2,3}$ ($2p \rightarrow 3d$) edges of $3d$ transition elements, the large $2p$ spin-orbit interaction couples very effectively the angular momentum of the photon to the electron spin. RIXS probes excitations with mixed charge and spin character across [9] or inside the Mott-gap [10]. Pure spin-flip excitations are also possible, as predicted theoretically [11] and first confirmed for NiO [12]. In the cuprates, dispersive ΔS=0 excitations have been observed in LCO both at the Cu K ($1s$) [13] and L_3 [14] edges, and in the ladder compound $Sr_{14}Cu_{24}O_{41}$ [15]. More recent theoretical and experimental work has shown that $L_{2,3}$ edge RIXS can be used to map the dispersion of single magnons in 2D cuprates [16]. Therefore x-rays are an interesting alternative to neutrons, with the noticeable advantage that RIXS can be performed also on sub-mm^3 samples. We have utilized these capabilities to study the largely unexplored magnon spectrum in SCOC.

Measurements were performed at the SAXES end station of the ADRESS beam line of the Swiss Light Source (SLS) [17]. Single crystals (4×4×0.5 mm^3) grown from the flux with the c-axis perpendicular to the large surface, and characterized by x-ray and neutron diffraction, were mounted on a flow cryostat. They were oriented with the c-axis and either

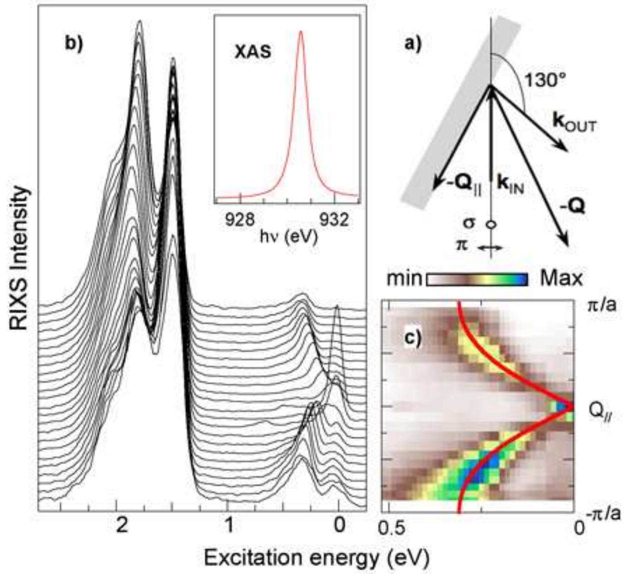

FIG. 1: (color online) (a) Schematics of the scattering geometry. (b) Cu L_3 RIXS spectra (T=15 K) along the (100) direction. The incident energy is set at the maximum of the XAS line shape (inset). (c) Intensity map extracted from panel (b). The red line is the spin-wave dispersion for the NN Heisenberg model and J=130 meV.

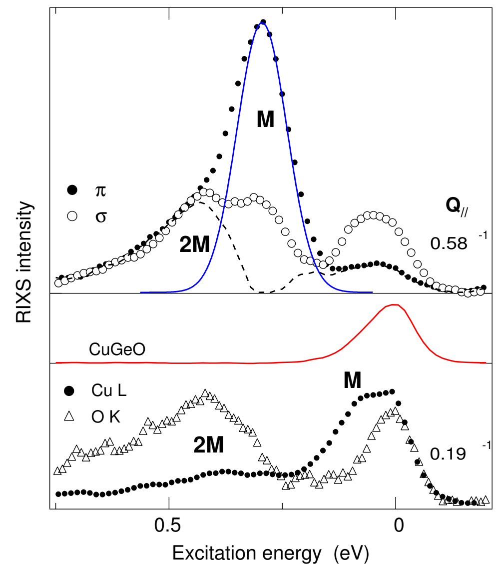

FIG. 2: (color online) (top) RIXS spectra of SCOC for σ and π polarization and $Q_{\|}$=0.58 Å^{-1} along (100). The dashed line is the difference between the π spectrum and the gaussian line shape (M, solid blue line) representing the single-magnon contribution. (middle) RIXS spectrum of $CuGeO_3$. (bottom) Comparison of Cu L-edge and O K-edge RIXS for the same $Q_{\|}$=0.19 Å^{-1}.

the (100) or the (110) directions in the horizontal scattering plane. By adjusting the undulator, data were taken with incoming polarization either perpendicular (σ) or within (π) this plane. The incident energy was $\hbar\omega_{in}$=930.6 eV, at the maximum of the L_3 ($2p_{3/2}$) absorption (XAS) line shape (Fig. 1b, inset). At the scattering angle of 130° the transferred momentum was $\|\mathbf{Q}\|$=0.85 Å^{-1}. By a rotation around a vertical axis, the c-axis described in the horizontal plane an angle of $-60°$ (5° grazing incidence) to 60° (5° grazing emission) from the specular reflection condition ($c \parallel \mathbf{Q}$). The projection $Q_{\|}$ of $\mathbf{Q}$ on the ab plane varied in the range $\pm$ 0.73 Å^{-1} ($\pm$ 0.92 π/a). The combined energy resolution was ΔE=130 meV, and the accuracy on the energy zero was $\pm$ 7 meV, as determined from the elastic peak measured on a co-planar polycrystalline carbon sample. The momentum resolution, determined by the detector size, was better than $\pm 2.5\times10^{-3}(\pi/a)$. Post-cleaving in situ or in air produced very similar results, confirming the good bulk sensitivity of L-edge RIXS.

Figure 1b is an overview of the data along the (100) direction for π-polarization. The data for σ polarization, albeit qualitatively similar, exhibit differences which are described below. All the spectra have been normalized to the same integrated intensity in the 1-2.5 eV energy range, to remove intensity variations due to the angular dependence of XAS, and any other angular or time dependence. The intrinsic angular-dependent intensity contains information on the ground state and on the scattering process [16], but it is not relevant for the present discussion. We verified that corrections for self-absorption, i.e. the partial re-absorption of the scattered beam, do not affect the excitation energies over the whole range of Fig. 1. The main spectral feature at ~1.5 eV is the manifold of optically-forbidden dd electron-hole excitations [10, 18]. In the 0-1.5 eV energy range, where no electronic excitations are expected, the spectra exhibit a loss feature dispersing upward symmetrically from $Q_{\|}$=0 (Fig. 1c). Near the zone boundary spectral weight extends beyond 300 meV, well above the highest phonon mode (70 meV) in SCOC [21]. Its maximum follows the calculated spin-wave dispersion for J=130 meV (red line, see below), strongly suggesting a magnetic origin of this feature.

This assignment is confirmed by a comparison with a $CuGeO_3$ sample, measured in the same conditions and for the same $Q_{\|}$ (Fig. 2). $CuGeO_3$ is also a Cu^{2+} S=1/2 insulator, but the energy scale of magnetic excitations extend only few tens of meV, and the RIXS line shape is close to that of the resolution-limited elastic spectrum from a carbon sample. Except for the slight asymmetry, attributed to phonons and low-energy magnons, the spectrum is completely clean in the energy range where SCOC show significant scattering. The following analysis shows that from the RIXS data it is possible to identify both the single-magnon dispersion, and a multi-magnon continuum.

A model independent analysis was performed by fitting the main peak of the spectrum to a resolution-limited gaussian line shape representing the single-magnon (M) contribution (Fig. 2 top). Subtracting this line shape from the raw spectrum yields asymmetric features (dashed line) on both sides of the magnon peak. The low energy feature contains the elastic line, phonon losses and possibly a residue due to the approximate magnon line shape. The higher-energy feature (2M) reflects two-magnon and higher-order excitations, which give rise to the continuum above the single-magnon dispersion curve in

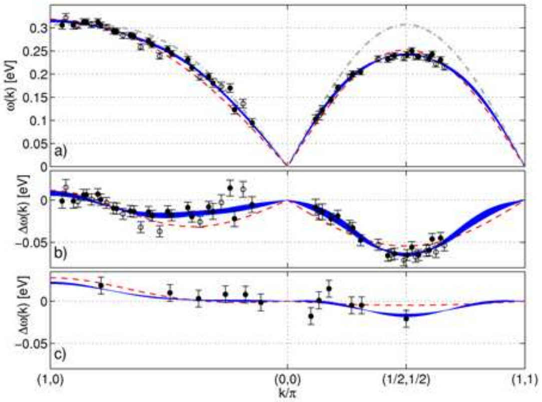

FIG. 3: (color online) a) Magnon energies extracted from the RIXS data. Open and closed symbols stem from 2 independent measurements on different samples. Dot-dashed line is a NN Heisenberg model with $J = 130$ meV. Red dashed line is a NN Hubbard model fit for $t = 0.261 \pm 0.004$ eV and $U = 1.59 \pm 0.04$ eV. Blue lines are the further neighbor Hubbard fits. b) same as a) with NN Heisenberg dispersion subtracted to better visualize details of the dispersion. The blue band shows the spread in dispersions obtained for fits with 1.9 eV$< U < 4$ eV. c) The fit to the neutron data on La_2CuO_4 from Coldea *et al.* [1].

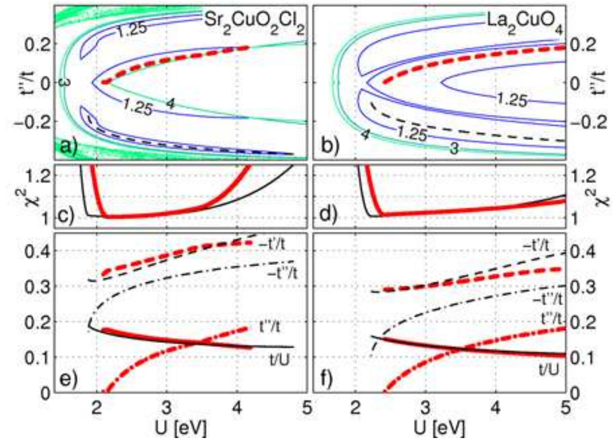

FIG. 4: (color online) Results of extended Hubbard model fits for SCOC (left) and LCO (right). a-b) χ^2 after fitting t and t' for fixed U and t''. Dashed lines mark the minima versus U, giving c-d) and e-f). c-d) χ^2 versus U, showing the range of U that our data can support. e-f) extracted hopping parameters t, t' and t'' as function of U. For given U, the uncertainty on the ts is around 5 meV. In all panels, thick red lines are for $t'' > 0$ and thin black lines for $t'' < 0$.

Fig. 1c. The details of this analysis have negligible impact on the extracted magnon energy. The typical uncertainty is ± 10 meV. For LCO, a similar phenomenological approach yields a magnon dispersion in excellent agreement with INS [16].

An interesting and unexplored aspect of RIXS is the possibility to separate single- and multi-magnon contributions by exploiting their different edge- and polarization-dependent cross sections, as illustrated in Fig. 2. The top panel shows spectra ($Q_\parallel = 0.58$ Å^{-1}) for two polarizations, normalized in the two-magnon region for ease of comparison. For σ polarization, the intensity of the single-magnon peak is strongly reduced with respect to the two-magnon continuum. The bottom panel compares Cu L_3 edge and O K edge ($1s$, 530 eV; ΔE=60 meV) data, for the same $Q_\parallel$ (0.19 Å^{-1}). Similar to the Cu K-edge case, the O K edge response contains only the two-magnon continuum, which was suggested by previous experiments[19, 20], and is now clearly resolved around 0.4 eV for this $Q_\parallel$. By contrast, the L_3 line shape exhibits a prominent single magnon loss at ~ 0.1 eV.

The Q-dependence of the magnon energy extracted from the data of Fig. 1, and from similar data for the (110) direction and two different samples, is summarized in Fig. 3. In the (100) direction data for both $Q_\parallel > 0$ and $Q_\parallel < 0$ are collapsed on the same $(0,0) - (\pi, 0)$ branch. The RIXS data are consistent with the small-Q results from INS, but cover for the first time the full dispersion up to the boundary of the MBZ. They reveal a striking 70 meV difference between the magnon energies of 310 meV at (π,0) and 240 meV at ($\pi/2$,$\pi/2$). This can be compared with the smaller $\sim$20 meV dispersion in LCO [1]. Dispersion along the zone boundary in all cuprates is also predicted by recent theory, which however underestimates the (π,0) energy in SCOC by almost 50 meV [22].

For the simple S=1/2 2D Heisenberg model with NN exchange, linear spin-wave theory predicts a constant magnon energy $\hbar\omega$=2J along the MBZ boundary. First order quantum corrections uniformly renormalize the dispersion by a factor Z_c=1.18. Numerical results [23, 24] and neutron data on $Cu(DCOO)_2 \cdot 4D_2O$ [25, 26] have established that the magnon energy for purely NN exchange is actually 6% larger at ($\pi/2$,$\pi/2$) than at (π,0). The dispersion in Fig. 3 and in LCO is in the opposite direction to this quantum effect. It could be reproduced by adding freely adjustable further neighbor exchange interactions. However, the Heisenberg (spin-only) hamiltonian is the low-energy projection of an electronic system at half filling, and a better approach is to systematically consider higher orders to this projection. Indeed the dispersion in LCO [1] was described by projecting the one-band Hubbard model with effective Coulomb repulsion U to 4th order in the NN hopping t, giving rise to further neighbor exchange interactions J, $J' = J''$ and J_c. The same approach gives for SCOC a very low value of $U = 1.59 \pm 0.04$ eV and $t = 0.261 \pm 0.004$ eV. The parameter U of the single band Hubbard model does not represent the Coulomb repulsion U_{dd} between two $3d$ holes on the same Cu^{2+} site, but rather the much smaller charge transfer energy between the Cu and O sites. Nevertheless, U=1.6 eV is quite small, also compared with LCO. This indicates that the Hubbard model with only NN hopping has reached its limit, and a more plausible approach is to include further neighbor hoppings t' and t'' [27]. We therefore extended the analysis to 4th order in t, t' and t'' and find that this approach give a more reasonable range of U, is consistent with higher energy RIXS and ARPES, and provide better fits to the shape of the dispersion (Fig. 3b).

Magnetic excitations provide accurate information on the interactions, but do not directly probe U. A more direct probe of the effective U was found in the higher energy part of the RIXS Cu-K spectra from the sister compound $Ca_2CuO_2Cl_2$, where a 2.5-4 eV dispersive feature analyzed within the one-band Hubbard model was reported consistent with $U = 3.5$ eV [9]. However, both the experimental and the numerical accuracy of such determinations can be improved. Therefore, to render our results applicable also to more accurate future determinations of U, we performed fits as a function of fixed U, as summarized in Fig. 4. The dispersion is symmetric in the signs of t' and t'', and leads to two possible solutions with $t't'' < 0$ and $t't'' > 0$ respectively. In compliance with ARPES and theoretical estimates, we assume $t' < 0$, and lean towards $t'' > 0$. Both solutions for $t'' \lessgtr 0$ constrain U to the range from ~ 2 eV to ~ 4 eV, and give essentially the same t/U and t'/t, which depend only weakly upon the chosen U, respectively from 0.17 to 0.14 and from -0.31 to -0.41. Hence, our data provide strict constraints on the effective parameters that can be used in the one-band Hubbard model for SCOC: U larger than 1.9 eV; significant second neighbor hopping $|t'/t| > 0.31$; and a unique set of hopping parameters for a given U (Fig. 4e). *E.g.* taking $U = 3.5$ eV, we obtain $t/U = 0.140 \pm 0.004$, $t'/t = -0.41 \pm 0.01$ and $t''/t = 0.14 \pm 0.01$ or -0.34 ± 0.01. These parameters are roughly consistent with ARPES results from SCOC [28], which were described by $U = 3.5$ eV, $t = 0.35$ eV, $t'/t = -0.35$ and $t''/t = 0.22$, with the accuracy of the comparison likely set by the broad ARPES linewidth. Thereby, we have derived a consistent description within a single model of both spin-wave and ARPES spectra.

To gain insight into the origin of the zone-boundary dispersion, we performed the same extended Hubbard model analysis for LCO (Fig. 4 right), using the 10 K data by Coldea *et al.* [1]. Also for LCO we find that the spin-wave dispersion can be described by a larger U more compatible with higher energy probes, and that there is significant further neighbor hopping, albeit slightly weaker than in SCOC. This trend, and our quantitative hopping parameters, are consistent with recent LDA and LDA+U calculations [29, 30], confirming experimentally that the main effect of the apical atom (oxygen in LSCO, chlorine in SCOC) is to influence the further neighbor hopping terms t' and t''. For the projected Heisenberg hamiltonian, this means that the difference in spin-wave dispersion comes not from different main interactions J and J_c, but from the many additional further neighbor hopping paths and hence magnetic interactions. The existence of so-called 'ring exchange' J_c coupling 4 spins on a plaquette generated significant theoretical efforts to understand the consequences of this term. An important conclusion from our work is that this term is not unique and that many further interactions and larger 4-spin loops have similar weight.

In summary, we have employed RIXS to obtain qualitative and quantitative new insight into the magnetic excitation spectrum of the representative insulating cuprate material $Sr_2CuO_2Cl_2$. Measuring the full spin-wave spectrum, we found a large zone boundary dispersion, which we could reproduce with an extended t-t'-t''-U Hubbard model, placing quantitative constraints on the hopping parameters. Most notably, we demonstrate sizeable longer range hopping, and henceforth magnetic interactions. Our experiment and analysis provide a general method, requiring only small crystals, to address the hopping parameters in other cuprates.

The SAXES instrument at the ADRESS beamline of the Swiss Light Source was jointly built by Paul Scherrer Institut and Politecnico di Milano. We gratefully acknowledge discussions with M. Mourigal, M. Gingras, J.-Y. Delannoy, F. Vernay and B. Normand, and support from the Swiss NSF and the MaNEP NCCR.

[1] R. Coldea, S. M. Hayden *et al.*, Phys. Rev. Lett. **86**, 5377 (2001).
[2] M. A. Kastner, R. J. Birgenau *et al.*, Rev. Mod. Phys. **70**, 897 (1998).
[3] J. D. Perkins, R. J. Birgenau *et al.*, Phys. Rev. B **58**, 9390 (1998).
[4] J. Lorenzana and G. A. Sawatzky, Phys. Rev. Lett. **74**, 1864 (1995).
[5] Y. Tokura, S. Koshihara *et al.*, Phys. Rev. B **41**, 11657 (1990).
[6] G. Blumberg, P. Abbamonte *et al.*, Phys. Rev. B **53**, R11930 (1996).
[7] M. Greven, R. J. Birgenau *et al.*, Z. Phys. B **96**, 465 (1995).
[8] A. Kotani and S. Shin, Rev. Mod Phys. **73**, 203 (2001).
[9] M. Z. Hasan, E. D. Isaacs *et al.*, Science **288**, 1811 (2000).
[10] G. Ghiringhelli, N. B. Brookes *et al.*, Phys. Rev. Lett. **92**, 117406 (2004).
[11] F. M. F. de Groot, P. Kuiper, and G. A. Sawatzky, Phys. Rev. B **57**, 14584 (1998).
[12] G. Ghiringhelli, A. Piazzalunga *et al.*, Phys. Rev. Lett. **102**, 027401 (2009).
[13] J. P. Hill, G. Blumberg *et al.*, Phys. Rev. Lett. **100**, 097001 (2008).
[14] L. Braicovich *et al.*, Phys. Rev. Lett. **102**, 167401 (2009).
[15] J. Schlappa *et al.*, Phys. Rev. Lett. **103**, 047401 (2009).
[16] L. J. P. Ament, G. Ghiringhelli *et al.*, Phys. Rev. Lett. **103**, 117003 (2009); L. Braicovich *et al.*, Phys. Rev. Lett. **104**, 077002 (2010).
[17] V.N. Strocov, T. Schmitt *et al.*, arXiv:0911.2598; G. Ghiringhelli *et al.*, Rev. Scient. Instrum. **77**, 113108 (2006).
[18] P. Kuiper, J.-H. Guo *et al.*, Phys. Rev. Lett. **80**, 5204 (1998).
[19] Y. Harada *et al.*, Phys. Rev. B **66**, 165104 (2002).
[20] V. Bisogni, PhD Thesis, Politecnico di Milano (2010).
[21] A. Zibold, H. L. Liu *et al.*, Phys. Rev. B **53**, 11734 (1996).
[22] X. Wan, T. A. Maier, and S. Y. Savrasov, Phys. Rev. B **79**, 155114 (2009).
[23] R. R. P. Singh *et al.*, Phys. Rev. B **52**, R15695 (1995).
[24] O. F. Syljuasen and H. M. Rønnow, J. Phys.: Condens. Matt. **12**, L405 (2000).
[25] H. M. Rønnow, D. F. McMorrow *et al.*, Phys. Rev. Lett. **87**, 037202 (2001).
[26] N. B. Christensen, H. M. Rønnow *et al.*, Proc. Natl. Acad. Sci. U.S.A. **104**, 15264 (2007).
[27] J.-Y. P. Delannoy, M. J. P. Gingras *et al.*, Phys. Rev. B **79**, 235130 (2009); We have corrected typos and included missing terms, B. Dalla Piazza *et al.* in preparation.
[28] P. W. Leung, B. O. Wells, and R. G. Gooding , Phys. Rev. B **56**,

6320 (1997).
[29] E. Pavarini *et al.*, Phys. Rev. Lett. **87**, 047003 (2001).
[30] W.-G. Yin and W. Ku, Phys. Rev. B **79**, 214512 (2009).